Acta Cryst. (1981). A**37**, 378–382

Radii of Gyration and Scattering Curves of Hollow Bodies of Homogeneous Electron Density

BY YUZURU HIRAGI AND SHOJI IHARA

Institute for Chemical Research, Kyoto University, Gokasho, Uji 611, *Kyoto-fu, Japan*

(*Received* 17 *April* 1980; *accepted* 2 *December* 1980)

Abstract

A general procedure for the calculation of radii of gyration and scattering intensities of hollow triaxial bodies is proposed. By this method, equations for the radii of gyration and the scattering intensities of hollow bodies, *i.e.* isosceles triangular, rectangular and regular polygonal prisms, elliptic cylinder and ellipsoid, are obtained. Existing models are expressed as the limited case of present results. The scattering curves of regular polygonal prisms of more than six sides are practically the same as that of a column. The curves have a tendency to become less undulant according to the decrease in isotropy of the body shape and the size of the hollow.

1. Introduction

Many enzymes, including allosteric enzymes, consist of several component subunits which form the oligomeric (quaternary) structure. This structure is considered to be related to the unique function of these enzymes; a change of the oligomeric structure produces an alteration in the function (Klotz, Langerman & Darnell, 1970; Monaco, Crawford & Lipscomb, 1978). Small-angle scattering methods with X-ray, synchrotron and neutron radiation are most suited to the study of the structures and the structural changes of these enzymes in solution.

It is very likely that all oligomeric enzymes except dimers have a void at the centre. Current methods for the analysis of the scattering of oligomeric enzymes in solution are based on two types of models, the triaxial-body model and the model attained by the stacking of these triaxial bodies in a certain manner (Glatter, 1972). Although the latter method allows more detailed analysis, the procedure to obtain the best model directly is not simple and requires laborious work. It is, therefore, better to start with simpler triaxial-body models as the primary approximation and, making use of this result, to advance to detailed analysis.

There has, however, so far been no general procedure for performing the analysis with hollow triaxial bodies. Here we will discuss the generalized forms of radii of gyration and scattering intensities of hollow triaxial bodies of homogeneous electron density; existing forms will be expressed as a special case. Although an analytical method using the distance distribution function has been developed recently and its usefulness in the application to biological macromolecules has been shown (Glatter, 1979), we confine the discussion in this article to the scattering intensity for simplicity; the expression of the distance distribution function is simply obtained by Fourier transformation of the intensity.

2. General expression of the calculation

The square of the radii of gyration and the scattering amplitude of a homogeneous body at a fixed orientation are given by integrating the corresponding function in the domain of the body. Taking the origin inside the hollow, D_2, as is shown in Fig. 1, these values $\mathcal{J}$ are generally given as

$$\mathcal{J}=\frac{\int_D \rho(\mathbf{r})w(\mathbf{r})\,d\mathbf{r}}{\int_D \rho(\mathbf{r})\,d\mathbf{r}}=\frac{\int_{D_1} \rho(\mathbf{r})w(\mathbf{r})\,d\mathbf{r}-\int_{D_2} \rho(\mathbf{r})w(\mathbf{r})\,d\mathbf{r}}{\int_{D_1} \rho(\mathbf{r})\,d\mathbf{r}-\int_{D_2} \rho(\mathbf{r})\,d\mathbf{r}}, \quad (1)$$

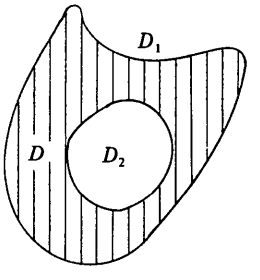

Fig. 1. The domain of integration of the hollow body D is expressed by the difference between the filled body D_1 and the hollow D_2.

0567-7394/81/030378-05$01.00

where $w(\mathbf{r}) = e^{is\mathbf{r}}$ for scattering amplitude or $w(\mathbf{r}) = \mathbf{r}^2$ for radii of gyration, $\rho(\mathbf{r})$ is the electron density of the body, $\mathbf{r}$ is the vector from the origin to an arbitrary point on D_1 or D_2, and $s = 4\pi \sin\theta/\lambda$ (2θ is the scattering angle, λ is the wavelength). Here discussion will be confined to a homogeneous body, *i.e.* $\rho(\mathbf{r})$ is the mean electron density of a body, a constant value. Then $\mathscr{I}$ is rewritten as

$$\mathscr{I} = (W_1 - W_2)/(V_1 - V_2), \tag{2}$$

with $W_i = \int_{D_i} w(\mathbf{r})\, d\mathbf{r}$ and $V_i = \int_{D_i} d\mathbf{r}$, the volume of the body ($i = 1$ or 2).

The calculation of (2) for a rectangular prism, an isosceles triangular prism, an elliptic cylinder and a regular polygonal prism has been performed. The dimensions of the bodies are shown in Fig. 2.

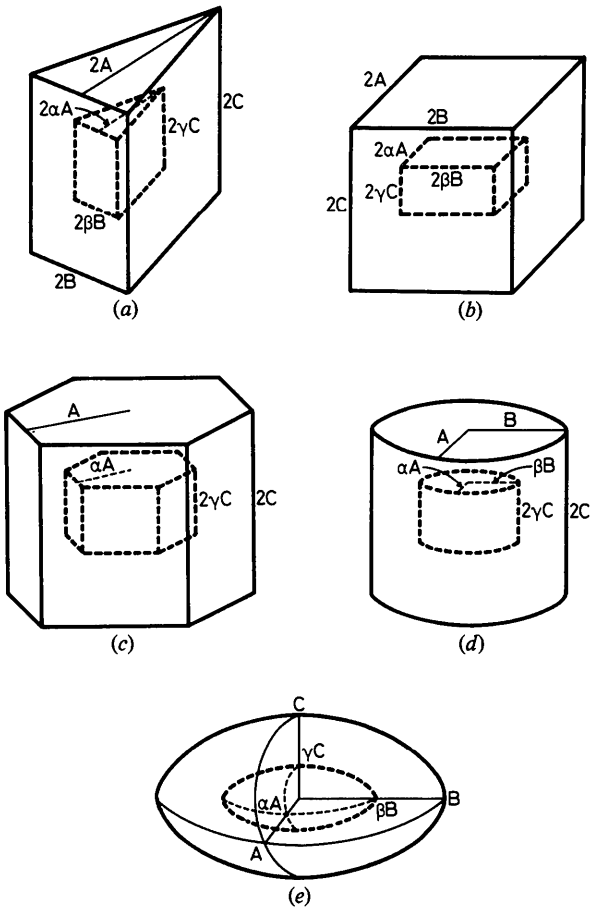

Fig. 2. Dimensions of the hollow triaxial bodies: (*a*) isosceles triangular prism; (*b*) rectangular prism; (*c*) regular polygonal prism of n sides (here represented by a hexagon); (*d*) elliptic cylinder; (*e*) ellipsoid.

3. Radii of gyration

The generalized form of the radii of gyration R_g will be derived from (2) with $w(\mathbf{r}) = \mathbf{r}^2$, and hence (for dimensions see Fig. 2)

$$W_i = \int_{-A}^{A}\int_{-B}^{B}\int_{-C}^{C} (x^2 + y^2 + z^2)\, dx\, dy\, dz, \tag{3}$$

$$V_i = \int_{-A}^{A}\int_{-B}^{B}\int_{-C}^{C} dx\, dy\, dz \tag{4}$$

in rectangular coordinates or with appropriate expressions in cylindrical or polar coordinates, depending on the model. With (3), the equations for the radii of gyration of the bodies with a hollow described by α, β and γ (the ratios of the inner to outer axes being $0 \le \alpha, \beta, \gamma \le 1$) are obtained.

(*a*) *Isosceles triangular prism*

$$R_g^2 = [4(1 - \alpha^3\beta\gamma)A^2 + 3(1 - \alpha\beta^3\gamma)B^2 + 6(1 - \alpha\beta\gamma^3)C^2]\,[18(1 - \alpha\beta\gamma)]^{-1}. \tag{5}$$

(*b*) *Rectangular prism*

$$R_g^2 = [(1 - \alpha^3\beta\gamma)A^2 + (1 - \alpha\beta^3\gamma)B^2 + (1 - \alpha\beta\gamma^3)C^2] \times [3(1 - \alpha\beta\gamma)]^{-1}. \tag{6}$$

(*c*) *Regular polygonal prism of n sides*

$$R_g^2 = \{(1 - \alpha^4\gamma)[3 + \tan^2(\pi/n)]A^2 + 2(1 - \alpha^2\gamma^3)C^2\} \times [6(1 - \alpha^2\gamma)]^{-1}. \tag{7}$$

(*e*) *Elliptic cylinder*

$$R_g^2 = [3(1 - \alpha^3\beta\gamma)A^2 + 3(1 - \alpha\beta^3\gamma)B^2 + 4(1 - \alpha\beta\gamma^3)C^2]\,[12(1 - \alpha\beta\gamma)]^{-1}. \tag{8}$$

(*e*) *Ellipsoid*

$$R_g^2 = [(1 - \alpha^3\beta\gamma)A^2 + (1 - \alpha\beta^3\gamma)B^2 + (1 - \alpha\beta\gamma^3)C^2] \times [5(1 - \alpha\beta\gamma)]^{-1}. \tag{9}$$

In all cases the R_g's of filled bodies are given by putting α, β and $\gamma = 0{\cdot}0$. The R_g's of rectangular prisms, polygonal prisms and elliptic cylinders are given by making $\gamma = 1{\cdot}0$, a circular pipe by putting $A = B$ and $\alpha = \beta$ in (8), a hollow sphere by making $A = B = C$ and $\alpha = \beta = \gamma$ in (9), and so forth.

4. Scattering intensities

The scattering amplitudes of filled bodies at a fixed orientation of zenith and azimuth angles θ, φ are given

by performing the calculation $\int w(\mathbf{r})\,\mathrm{d}\mathbf{r}$ with $w(\mathbf{r}) = e^{i\mathbf{s}\mathbf{r}}$. Rewrite the amplitudes as $F(A,B,C,s,\theta,\varphi)$ instead of W, and with $s_1 = s\sin\theta$, $s_2 = s\cos\theta$ and $\Psi_C = \sin(Cs_2)/(Cs_2)$, they are given by the following equations.

(*a*) *Isosceles triangle prism* (Bode, Engel & Winklmair, 1972)

$$V = 4ABC, \tag{10}$$

$$F = \frac{8ABC\exp\left(-i\frac{4}{3}As_1\cos\varphi\right)}{(B^2\sin^2\varphi - 4A^2\cos^2\varphi)\,s_1^2} \times \left\{\exp(i2As_1\cos\varphi)\left[2i\frac{A}{B}\cot\varphi\sin(Bs_1\sin\varphi) - \cos(Bs_1\sin\varphi)\right] + 1\right\}\Psi_C. \tag{11}$$

(*b*) *Rectangular prism* (Mittelbach & Porod, 1961*a*)

$$V = 8ABC, \tag{12}$$

$$F = 8ABC\left[\frac{\sin(As_1\cos\varphi)}{As_1\cos\varphi}\right]\left[\frac{\sin(Bs_1\sin\varphi)}{Bs_1\sin\varphi}\right]\Psi_C. \tag{13}$$

(*c*) *Regular polygonal prism of n sides**

$$V = 2nA^2C\tan(\pi/n), \tag{14}$$

$$F = 4A^2C\left\{\sum_{k=1}^{n} f_k\left(s_1, \varphi - \frac{2\pi}{n}k\right) \times \exp\left[iAs_1\cos\left(\varphi - \frac{2\pi}{n}k\right)\right]\right\}\Psi_C, \tag{15}$$

where

$$f_k = \left\{A^2s_1^2\left[\tan^2\frac{\pi}{n}\sin^2\left(\varphi - \frac{2k}{n}\pi\right) - \cos^2\varphi\right]\right\}^{-1} \times \left[\left\{i\cot\left(\varphi - \frac{2\pi}{n}k\right)\sin\left[s_1A\sin\left(\varphi - \frac{2\pi}{n}k\right)\right] - \tan\frac{\pi}{n}\cos\left(s_1A\tan\frac{\pi}{n}\sin\varphi\right)\right\} + \tan\frac{\pi}{n}\right]. \tag{16}$$

(*d*) *Elliptic cylinder* (Mittelbach & Porod, 1961*b*)

$$V = 2ABC, \tag{17}$$

$$F = \frac{4\pi J_1(s_1K)}{s_1K}\Psi_C, \tag{18}$$

where $K = [A^2\cos^2\varphi + B^2\sin^2\varphi]^{1/2}$ and J_1 is a Bessel function of first order.

* Full details of the calculations have been deposited with the British Library Lending Division as Supplementary Publication No. SUP 35861 (6 pp.). Copies may be obtained through The Executive Secretary, International Union of Crystallography, 5 Abbey Square, Chester CH1 2HU, England.

(*e*) *Ellipsoid* (Mittelbach & Porod, 1962)

$$V = \tfrac{4}{3}\pi ABC, \tag{19}$$

$$F = 4\pi\frac{\sin(sL) - sL\cos(sL)}{(sL)^3}, \tag{20}$$

where $L = [A^2\sin^2\theta\cos^2\varphi + B^2\sin^2\theta\sin^2\varphi + C^2\cos^2\theta]^{1/2}$.

As the normalized amplitude of a hollow body F_h is given by $F_h = (F_1 - F_2)/(V_1 - V_2)$ and the scattering intensity at fixed orientation I is given as the product of F_h and its complex conjugate F_h^*, namely $I(s,\theta,\varphi) = F_hF_h^*$, we get the observable intensity $J(s)$ which derives from the scattering by particles in random orientations through the integration of I with respect to θ and φ,

$$J(s) = \frac{\int_{\theta=0}^{\pi}\int_{\varphi=0}^{2\pi} I(s,\theta,\varphi)\sin\theta\,\mathrm{d}\theta\,\mathrm{d}\varphi}{\int_0^{\pi}\int_0^{2\pi}\sin\theta\,\mathrm{d}\theta\,\mathrm{d}\varphi} \tag{21}$$

or with the size of the hollow αA, βB and γC, this can be rewritten as

$$J(s) = \int_0^{\pi}\int_0^{2\pi} |F_1(A,B,C,s,\theta,\varphi) - F_2(\alpha A,\beta B,\gamma C,s,\theta,\varphi)|^2\sin\theta\,\mathrm{d}\theta\,\mathrm{d}\varphi \times [4\pi|V_1(A,B,C) - V_2(\alpha A,\beta B,\gamma C)|^2]^{-1}. \tag{22}$$

By the symmetry of the models, the range of the integrations can be reduced. For all models, a range from 0 to $\pi/2$ suffices for the integration of $|F_1 - F_2|^2\sin\theta$ with respect to θ. Reducible ranges of the integration with respect to φ depend on the model. For a rectangular prism, elliptic cylinder and ellipsoid, it is from 0 to $\pi/2$; for a triangular prism from 0 to π and for a regular polygonal prism from 0 to π/n. To obtain the normalized values of $J(s)$, the results of integrations are to be multiplied respectively by eight for rectangular prism, elliptic cylinder and ellipsoid; by four for triangular prism and by $2n$ for regular polygonal prisms.

5. Results of computation and discussion

Computation of the scattering curves with different bodies and shapes are performed with a FACOM M-160AD computer using the FACOM SSL (Scientific Subroutine Library) subroutines. The program is written in Fortran; a copy is available upon request, either in the form of printout or recorded magnetic tape in EBCDIC code. Some of the results are shown in Figs. 3–6. For ease of comparison of different models,

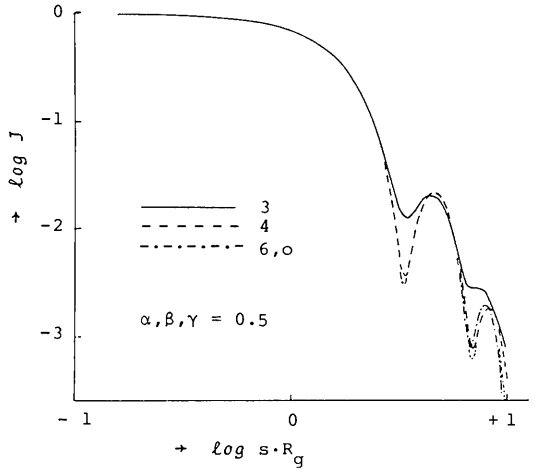

Fig. 3. Scattering curves of prisms with the ratio of cross section to height = $\pi/1{\cdot}0$ and degree of hollowness = 1/8. Figures represent 3: triangular; 4: square, 6: hexagonal prisms, and O: column.

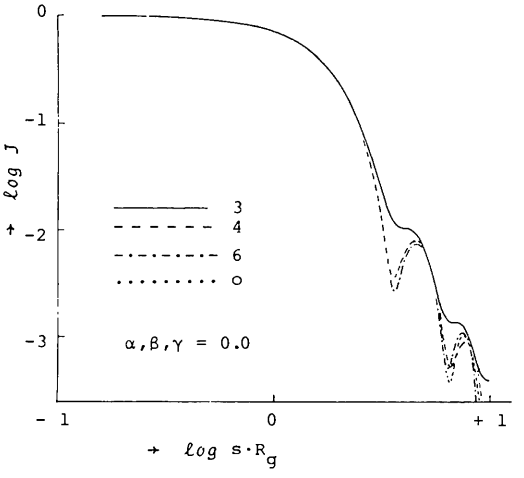

Fig. 4. Scattering curves of filled prisms. Cross section/height = $\pi/1{\cdot}0$.

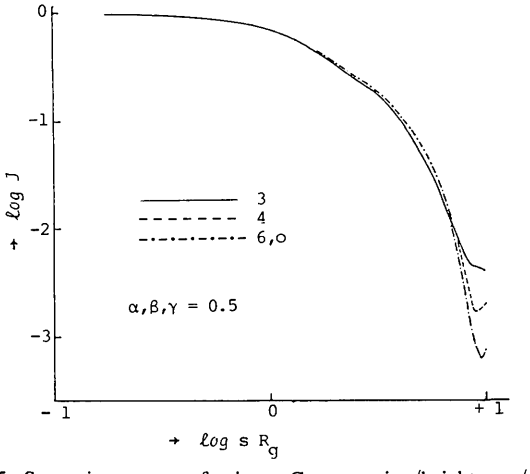

Fig. 5. Scattering curves of prisms. Cross section/height = $\pi/4{\cdot}0$ and degree of hollowness = 1/8.

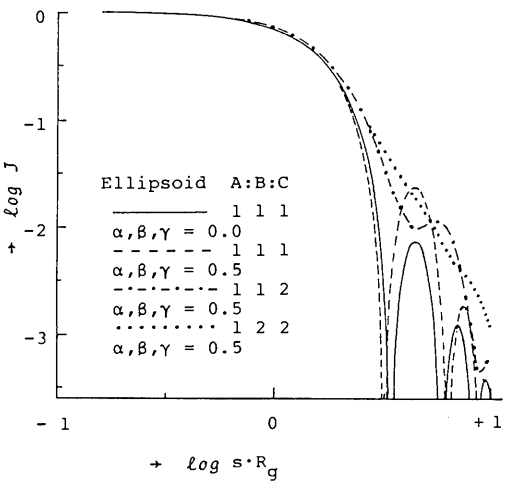

Fig. 6. Scattering curves of an ellipsoid with different axial ratios and degree of hollowness.

the radius of gyration R_g, which is the value obtainable directly from the experiments, is kept at 50 Å throughout and the ratio of the cross section to the height of the prism is kept constant in each figure.

It is a matter of concern to what degree one can distinguish similar bodies, especially prisms, from the scattering curves. As can be deduced from Figs. 3, 4 and 5, the triangular prism has remarkably different, less undulant, scattering curves to those of the others. We are also able to distinguish the rectangular prism, if the measurements are made carefully. It would not be impossible to discriminate the hexagonal prism from the column if the measured intensities $J(s)$ had very small errors up to considerably high angles and are plotted on an enlarged scale in order to clarify the small differences in the curve. It seems meaningless to analyse the polygonal prism of more than six sides, because their scattering curves practically show no difference from the column. In outline, the point of the argument is the same irrespective of the hollowness and the cross-section/height ratio.

Comparing Fig. 3 with Fig. 4 or Fig. 6, we can see the effect of the size of the hollow, which depends on the parameters α, β and γ, on the scattering curve. The tendency is that the larger the hollow is, the deeper the minima and the higher the maxima of a scattering curve become. However, the variance of the features of a curve is not very remarkable in this case compared with the change of ratios of axes; the curves have some similarity.

The authors are grateful to Professor K. Katayama for discussions and Dr K. Kajiwara for reading the manuscript.

References

BODE, W., ENGEL, J. & WINKLMAIR, D. (1972). *Eur. J. Biochem.* **26**, 313–327.

GLATTER, O. (1972). *Acta Phys. Austriaca*, **36**, 307–315.
GLATTER, O. (1979). *J. Appl. Cryst.* **12**, 166–175.
KLOTZ, I. M., LANGERMAN, N. R. & DARNELL, D. W. (1970). *Ann. Rev. Biochem.* **39**, 25–62.
MITTELBACH, P. & POROD, G. (1961*a*). *Acta Phys. Austriaca*, **14**, 185–211.
MITTELBACH, P. & POROD, G. (1961*b*). *Acta Phys. Austriaca*, **14**, 405–439.
MITTELBACH, P. & POROD, G. (1962). *Acta Phys. Austriaca*, **15**, 122–147.
MONACO, H. L., CRAWFORD, J. L. & LIPSCOMB, W. N. (1978). *Proc. Natl Acad. Sci. USA*, **75**, 5276–5280.

Acta Cryst. (1981). A**37**, 382–390

Absolute Thermal Diffuse Scattering Measurements. I

BY JOHN S. REID

Department of Natural Philosophy, The University, Aberdeen AB9 2UE, Scotland

(*Received* 30 *August* 1980; *accepted* 5 *December* 1980)

Abstract

Consideration is given to the quantities required to convert measured X-ray intensities into absolute units for comparison with theoretical predictions. Attention is focused on the instrumental resolution correction and the factors of incident beam spread and wavelength range, crystal mosaic spread, and detector size and efficiency that contribute to the spread of wavevectors necessarily sampled in a given measurement. A scheme is presented for handling each of these factors with confidence and generally without any assumptions as to their simple analytic form. A set of auxiliary measurements is described which enables a practical amount of data to be collected for the required convolutions. The scheme also provides a simple method for aligning the apparatus in a known way. Some numerical examples are given of the effect of the factors on smearing the scattering from KCl in our apparatus.

Introduction

There is a continuing interest in X-ray thermal diffuse scattering (TDS) but the technique of making absolute measurements of TDS cross sections has in the past acquired a reputation for difficulty, one which it does not really deserve. However, it is a technique in which it is of the utmost importance that attention be given to quite a number of details before confidence can be placed in the final results. This importance has been emphasized from time to time by recurring controversy on the accuracy of published experimentally measured phonon scattering intensities. Techniques have changed over the years and therefore, in the interests of discussing points which generally have been neglected in the literature, an account of experimental considerations relevant to obtaining reliable absolute measurements will be presented. A description of our own methods is long overdue because no systematic account has been given, although some aspects have been reported in earlier papers by Buyers & Smith (1966), Pirie & Smith (1968) and Peterson & Smith (1972).

Of course, there is essentially no difference between measuring thermal diffuse scattering and other diffuse scattering caused by disorder or defects, for the scattered photons are not labelled by the scattering process. Hence, the method should be applicable to diffuse scattering in general. However, where theoretical intensities are required, those relevant to thermal scattering will be discussed and numerical values quoted from thermal scattering cross sections. This reflects the limits for which the methods have been tried and tested.

Part I of this account, excepting this introduction, is concerned with recent developments in evaluating the instrumental resolution function, an essential step in the analysis of measurements. Discussion of other aspects of technique is left to part II (Pirie & Reid, 1981) which also presents new absolute measurements for some alkali halides.

Absolute TDS measurements are made on single crystals. The scattering vector **K** is always chosen to be intermediate between reciprocal-lattice points because, apart from using the Mössbauer effect, there is no way of measuring the TDS under Bragg reflections. The only crystal shape in which absorption in an inhomogeneous beam can be handled with complete confidence is a parallel-sided slab where the face presented to the incident beam is large enough to intercept the entire beam. This shape will be assumed, though the procedure that will be described can be extended to handle any sample shape.

Much has been said on the relative merits of photographic recording *versus* direct photon counting

0567-7394/81/030382-09$01.00